Available online at www.sciencedirect.com
ScienceDirect
Bioorganic & Medicinal Chemistry Letters 17 (2007) 5677–5682
Bioorganic & Medicinal Chemistry Letters

Kinesin spindle protein (KSP) inhibitors. Part 8: Design and synthesis of 1,4-diaryl-4,5-dihydropyrazoles as potent inhibitors of the mitotic kinesin KSP

Anthony J. Roecker,[a,*] Paul J. Coleman,[a] Swati P. Mercer,[a] John D. Schreier,[a] Carolyn A. Buser,[b] Eileen S. Walsh,[b] Kelly Hamilton,[b] Robert B. Lobell,[b] Weikang Tao,[b] Ronald E. Diehl,[b] Vicki J. South,[b] Joseph P. Davide,[b] Nancy E. Kohl,[b] Youwei Yan,[c] Lawrence C. Kuo,[c] Chunze Li,[d] Carmen Fernandez-Metzler,[d] Elizabeth A. Mahan,[d] Thomayant Prueksaritanont[d] and George D. Hartman[a]

[a]*Department of Medicinal Chemistry, Merck Research Laboratories, PO Box 4, Sumneytown Pike, West Point, PA 19486, USA*
[b]*Department of Cancer Research, Merck Research Laboratories, PO Box 4, Sumneytown Pike, West Point, PA 19486, USA*
[c]*Department of Structural Biology, Merck Research Laboratories, PO Box 4, Sumneytown Pike, West Point, PA 19486, USA*
[d]*Department of Drug Metabolism, Merck Research Laboratories, PO Box 4, Sumneytown Pike, West Point, PA 19486, USA*

Received 30 May 2007; revised 16 July 2007; accepted 17 July 2007
Available online 21 August 2007

Abstract—Inspired by previous efforts in the pyrazolobenzoxazine class of KSP inhibitors, the design and synthesis of 1,4-diaryl-4,5-dihydropyrazole inhibitors of KSP are described. Crystallographic evidence of binding mode and in vivo potency data is also highlighted.

In the preceding communications, several classes of KSP inhibitors, including dihydropyrazoles, dihydropyrroles, and pyrazolobenzoxazines, have been described.[1] Several members of each of these classes of compounds have demonstrated excellent biochemical and cellular potencies against KSP, aqueous solubility, limited susceptibility to P-glycoprotein-mediated efflux, and potency in a xenograft mouse model of cancer. Inspired from the recent forays into the dihydropyrazolobenzoxazine class of compounds (**1**, Fig. 1), herein we describe the design and synthesis of a novel class of KSP inhibitors, namely the 1,4-diaryl-4,5-dihydropyrazoles.[2] This novel class of KSP inhibitors maintained the aforementioned properties of the previous classes of KSP inhibitors as well as comparable potency in vivo. Crystallographic evidence of the similarities in binding mode of the dihydropyrazolobenzoxazine and 1,4-dia-

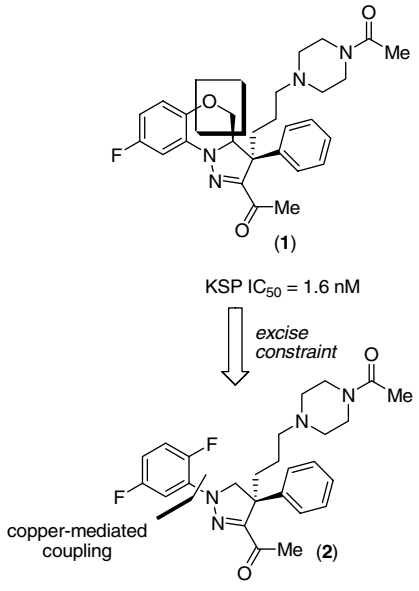

Figure 1. Potent dihydropyrazolobenzoxazine KSP inhibitor (**1**) inspired efforts to synthesize and study its 1,4-diaryl-4,5-dihydropyrazole analog (**2**).

Keywords: KSP inhibitors; Antimitotics; Pgp; Kinesins; 1,4-Diaryl-4,5-dihydropyrazoles; Copper-mediated N-arylation; Kinesin spindle protein; Cancer.
* Corresponding author. Tel.: +1 215 652 8257; fax: +1 215 652 7310; e-mail: anthony_roecker@merck.com

0960-894X/$ - see front matter © 2007 Elsevier Ltd. All rights reserved.
doi:10.1016/j.bmcl.2007.07.074

ryl-4,5-dihydropyrazole class of inhibitors to an allosteric site of the KSP enzyme will also be demonstrated.

Chemistry. Inspiration for the synthesis of 1,4-diaryl-4,5-dihydropyrazoles as KSP inhibitors was derived from compound **1** as shown in Figure 1. Compound **1** is a highly potent member of the dihydropyrazolobenzoxazine class of KSP inhibitors (IC_{50} = 1.6 nM), the details of which are covered in the preceding publication.[1g] Excision of the central methyleneoxy constraint affords a target 1,4-diaryl-4,5-dihydropyrazole (**2**) containing only a single stereocenter. This seemingly simplified structure could not be easily synthesized in a manner analogous to compound **1**. Compound **1** was synthesized through an intramolecular [3 + 2] cycloaddition utilizing the methyleneoxy subunit as a linker.[1g] The application of an intermolecular version of this cycloaddition process to the synthesis of **2** was daunting,[3] thus an alternative synthetic approach was sought.

One novel approach relied on a copper-mediated N-arylation using pyrazolines and boronic acids for the formation of the key pyrazoline-aryl bond. First disclosed by Lam, Chan, and Evans, this methodology allows a variety of heterocyclic nucleophiles including anilines, anilides, imidazoles, pyrazoles, triazoles, and indazoles to be arylated by boronic acids in good to excellent yields.[4] However, the use of pyrazolines as nucleophiles in these copper-mediated reactions has been scarce and only recently has progress been made utilizing di- and triarylbismuth reagents.[5] With this concept in mind we began an effort to synthesize the 1,4-diaryl-4,5-dihydropyrazole targets such as **2**.

The implementation of our strategy is shown in Scheme 1. The synthesis in racemic form begins with the addition of diazomethane to methyl cinnamate (**3**) to afford pyrazoline **4** in near quantitative yield and as a single regioisomer as precedented in the literature.[6] The pyrazoline (**4**) was then exposed to the requisite boronic acid, copper (II) acetate, and triethylamine in dichloromethane in air overnight to yield arylated products **5**. Although the yields were low, the only byproduct was retro-cycloaddition resulting in re-isolation of methyl-cinnamate which was readily separated from N-arylpyrazoline products (**5**). Compound **5** was then allylated (LHMDS, allyl bromide)[7] in good yield to afford **6** and subsequently transformed into the Weinreb amide (**7**) in a two-step procedure. Compound **7** was treated with 9-BBN followed by oxidation to afford regioselective hydroboration product **8**. Compounds of type **8** were then advanced to the final targets (**10**) through transformation of the Weinreb amide to a methyl ketone (MeLi), oxidation of the primary alcohol (Dess–Martin periodinane), and reductive amination with various amines.

In vitro SAR and X-ray crystallographic analysis. Our investigations into the effect of the amine on the intrinsic[8] and cellular potency[9] of 1,4-diaryl-4,5-dihydropyrazoles are shown in Table 1. In general, the intrinsic potency of the compounds did not vary greatly with modulation of the amine. It is notable that compound

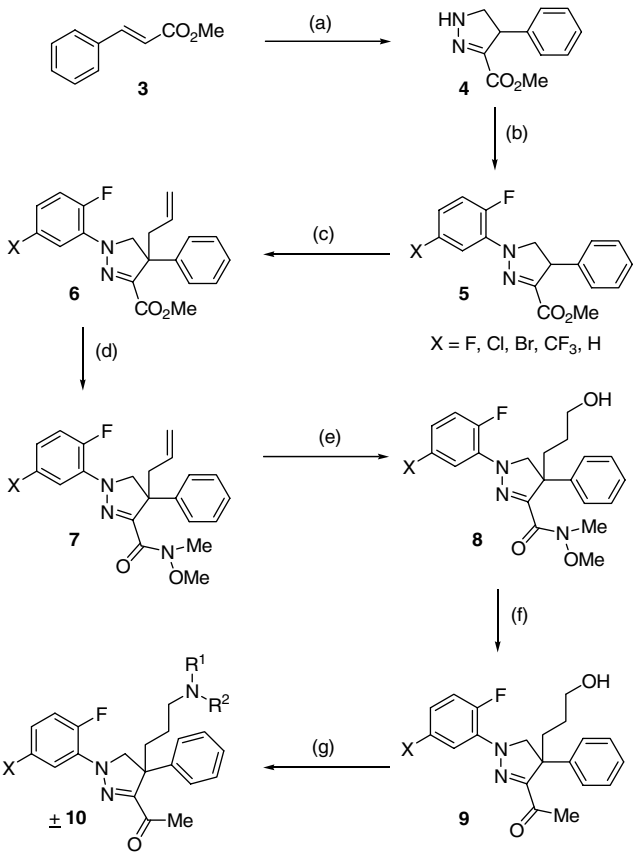

Scheme 1. General synthesis of 1,4-diaryl-4,5-dihydropyrazole KSP inhibitors. Reagents and reaction conditions: (a) CH_2N_2, Et_2O, 0–25 °C, 12 h, 98%; (b) $ArB(OH)_2$, $Cu(OAc)_2$, Et_3N, CH_2Cl_2, 24 h, 5–27%; (c) LHMDS, allyl bromide, −78 to −5 °C, THF, 2 h, 50–72%; (d) 1.0 M NaOH, 25 °C, THF, 24 h, aqueous workup, then MeN(OMe)HCl, EDC, HOAt, Et_3N, THF:DMF (1:1), 16 h, 80–94%; (e) 9-BBN, THF, 55 °C, then H_2O_2, NaOH, 25 °C, 1 h, 58–72%; (f) MeLi, THF, 0 °C, 1 h, 38–67%; (g) Dess–Martin periodinane, $NaHCO_3$, CH_2Cl_2, 1 h, then R^1R^2NH, $NaBH(OAc)_3$, Et_3N, 1,2-dichloroethane, 2 h, 54–80%.

2 bearing the same amine as dihydropyrazolobenzoxazine **1** maintains excellent intrinsic potency (3.8 nM) while suffering a 16-fold loss in cellular potency (78 nM). Modulation of the amine to a tertiary heterocyclic amine (**11**) or thiomorpholine dioxide (**12**) afforded compounds with diminished cellular potency as compared to **2**. Potency in cells was regained when the acetylpiperazine was replaced with various tertiary amines such as morpholine **12** (53 nM), 3-fluoroazetidine **14** (40 nM), pyrrolidine **15** (15 nM), and bridged morpholine **16** (11 nM). The best substituent in the subset tested was dimethylamine (**17**) having biochemical potency of 2.1 nM and cellular potency of 9.4 nM.

From previous work in the 3,5-diaryl-4,5-dihydropyrazole series,[1a] it was shown that the 5-position of the aromatic ring could have a significant effect on KSP potency. The results of a similar investigation in the 1,4-diaryl-4,5-dihydropyrazole series are shown in Table 2. Compounds containing a halogen at the 5-position (**2**, **18**, and **19**) showed good intrinsic potency and up to a twofold improvement in cellular activity as shown for

Table 1. Sidechain amine SAR

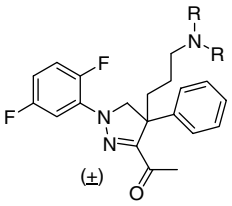

Compound	Amine	KSP IC_{50}[a] (nM)	Cell EC_{50}[a] (nM)
2	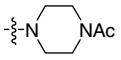	3.8	78
11	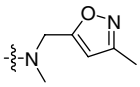	4.0	567
12	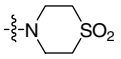	16.5	138
13		4.2	53
14	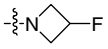	5.2	40
15		3.8	15
16[b]		1.2	11
17		2.1	9.4

[a] See Refs. 8,9 for the details of these assays. All compounds listed were assayed as racemates.
[b] Approximately 1:1 mixture of diastereomers.

compound **19** (38 nM). Deletion of the 5-position substituent afforded a sixfold decrease in intrinsic potency concomitant with a fivefold decrease in cell potency. Incorporation of a trifluoromethyl (**21**) group was also deleterious with respect to potency. Finally, changing the 5-position fluorine to a methyl group afforded compound **22** which gave a twofold and threefold improvement in intrinsic (2.0 nM) and cellular (27 nM) potency as compared to **2**.

With these results in hand, a more advanced target was sought containing the optimal substituents in both the western aryl ring and the amine substituent. The synthesis of such a compound is shown in Scheme 2. Advanced intermediate **23** (see compound **8**, Scheme 1) was treated under Stille coupling conditions [tetramethyltin, LiCl, and $Pd(PPh_3)_4$], and the Weinreb amide was subsequently transformed into the methyl ketone via the action of methyllithium affording **24** in acceptable yield. Oxidation of the primary alcohol in **24** with Dess–Martin reagent and reductive amination with dimethylamine gave **25**. Compound **25** was then separated into its enantiomers using a ChiralPak AD column to afford the active enantiomer shown as *R*-(+)-**25**.[10]

Table 2. SAR of the 5-position of the western aryl ring

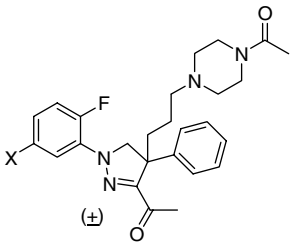

Compound	X	KSP IC_{50}[a] (nM)	Cell EC_{50}[a] (nM)
2	F	3.8	78
18	Cl	3.9	46
19	Br	4.7	38
20	H	21.8	368
21	CF_3	10.1	208
22	CH_3	2.0	27

[a] See Refs. 8,9 for the details of these assays. All compounds listed were assayed as racemates.

The determination of the stereochemistry of **25** was aided by the high resolution crystal structure of compound **22** (synthesized in an analogous fashion to **25**, Scheme 2) in an allosteric binding site of KSP.[11] Compound **22** in racemic form was co-crystallized with KSP as shown in Figure 2, and only the *R*-antipode docks in the allosteric binding site. As expected, compound **1** and compound **22** show many similar interac-

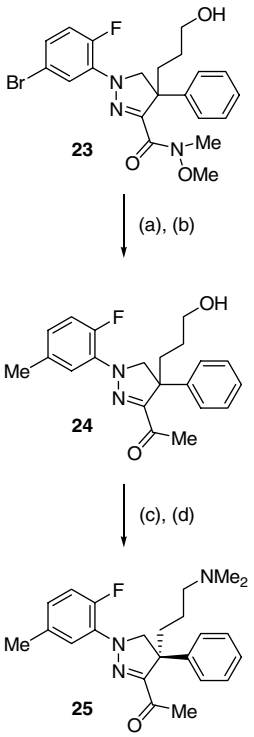

Scheme 2. Synthesis of the 5-methyl derivative on the western aryl ring (**25**). Reagents and reaction conditions: (a) Me_4Sn, LiCl, $Pd(PPh_3)_4$, DMF, 105 °C, 1 h, 93%; (b) MeLi, THF, 0 °C, 1 h, 64%; (c) Dess–Martin periodinane, $NaHCO_3$, CH_2Cl_2, 1 h, then dimethylamine, $NaBH(OAc)_3$, Et_3N, 1,2-dichloroethane, 2 h, 53%; (d) ChiralPak AD separation.

tions with the allosteric binding site of the enzyme: (1) the key hydrophobic interactions of both aryl rings; (2) the projection of the methyl ketone moiety into a solvent exposed area of the enzyme; and (3) the use of the unoccupied space above the plane of the core of the compounds by a tethered amine. By analogy with compound **22** as well as many other Merck KSP inhibitors, compound **25** was assigned the stereochemistry of *R*. With enantiomerically pure **25** in hand we sought to study its in vitro and in vivo properties.

*In vitro and in vivo comparison of **1** and **25**.* The key data for the comparison of compounds **1** and **25** are shown in Table 3. Compared to compound **1**, compound **25** demonstrated excellent activity giving an eightfold increase in intrinsic potency. Moreover, the KSP IC_{50} of 0.2 nM represents significant additivity of the amine and western aryl ring SAR. Compound **25** was particularly potent in cells (3.2 nM) showing approximately equivalent potency to dihydropyrrolobenoxazine **1** (5.0 nM). The cellular activity also shows additivity with respect to compounds **17** and **22**. Compound **25** maintained adequate aqueous solubility at moderate pH. Next, we studied the hERG inhibition properties, Pgp susceptibility, and in vivo efficacy of compound **25** as compared with compound **1**.

As discussed in the two preceding letters, we have chosen to target compounds that are similarly potent in Pgp-overexpressing cell lines and normal KB cell lines with the hope of avoiding resistance due to Pgp-mediated efflux. A detailed analysis of Pgp and KSP inhibitors has been published from our group.[1e] Compound **25** showed an MDR ratio of 1.6 which compares very favorably to compound **1** (1.0).[12] A second important design criterion of KSP inhibitors has been to minimize affinity for hERG with the hope of diminishing the possibility of cardiotoxicity. Although compound **25** has approximately a threefold increase in binding affinity for hERG as compared to compound **1**, the eightfold increase in KSP IC_{50} actually increases the off-target window (hERG IC_{50}/KSP IC_{50}) from approximately 6000 to 15,000.[13] Finally, the in vivo potency of compound **25** was measured in a nude mouse model containing a human xenograft from an A2780 cell line (in vivo mitotic arrest assay).[14] Compound **25**, dosed as a solution in pH 4 buffer, provides maximum induction of phospho-histone H3 with a dose of 3.5 mpk and 67 nM plasma concentrations. This level of in vivo potency may translate well in humans as compound **25** has similar protein binding in mouse (93%) and human (96%) plasma. This result also represents comparable potency with respect to compound **1** which demonstrated a similar in vivo effect with a plasma concentration of 100 nM.

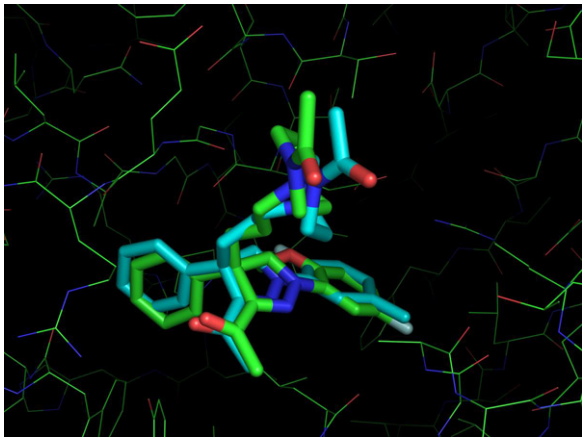

Figure 2. Overlay of X-ray structures of *R*-**22**-ADP (cyan) and **1**-ADP (green) in the allosteric KSP binding site.

Table 3. Comparison of key data for compounds **1** and **25**

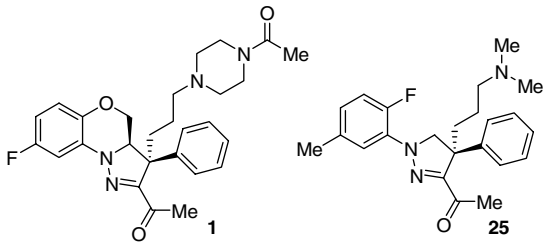

Property	1	25
KSP IC_{50}[a] (nM)	1.6	0.2
Cell EC_{50}[a] (nM)	5.0	3.2
Solubility (pH 4, mg/mL)	>4	>4
MDR ratio[b]	1.0	1.6
hERG IC_{50}[c] (nM)	10,000	3036
M2B (~EC_{99}; nM)[d]	100	67

[a] See Refs. 8,9 for the details of these assays.
[b] See Ref. 12 for a more detailed discussion of this assay.
[c] See Ref. 13 for an assay description and relevant references therein.
[d] See Ref. 14 for a discussion of this assay.

In conclusion, we have described a novel series of 1,4-diaryl-4,5-dihydropyrazole KSP inhibitors designed from the dihydropyrazolobenzoxazine class of KSP inhibitors. These compounds were synthesized using a novel approach through a copper-mediated arylation reaction between pyrazolines and aryl boronic acids. The SAR between the western aryl ring and sidechain amine was additive and prompted the synthesis of compound **25** in enantiopure form. Compound **25** was exceptionally potent with good cellular activity, demonstrated aqueous solubility at moderate pH, showed good potency in Pgp-overexpressing cells, and demonstrated full mitotic arrest in a mouse xenograft model of cancer with low plasma exposure. Taken together, the last three letters have described three distinct classes of KSP inhibitors that possess good to excellent intrinsic potency, aqueous solubility, low MDR ratios, limited hERG affinity, and excellent in vivo potency. Additional series of KSP inhibitors will be the topic of future publications and will be described in due course.

Acknowledgments

The authors thank Dr. Chuck Ross, Dr. Harri Ramjit, and Joan Murphy for high resolution mass spectral

analyses. The authors also thank Maricel Torrent for assistance with the figures in this manuscript.

References and notes

1. (a) Cox, C. D.; Breslin, M. J.; Mariano, B. J.; Coleman, P. J.; Buser, C. A.; Walsh, E. S.; Hamilton, K.; Huber, H. E.; Kohl, N. E.; Torrent, M.; Yan, Y.; Kuo, L. C.; Hartman, G. D. *Bioorg. Med. Chem. Lett.* **2005**, *15*, 2041; (b) Fraley, M. E.; Garbaccio, R. M.; Arrington, K. L.; Hoffman, W. F.; Tasber, E. S.; Coleman, P. J.; Buser, C. A.; Walsh, E. S.; Hamilton, K.; Schaber, M. D.; Lobell, R. B.; Tao, W.; South, V. J.; Yan, Y.; Kuo, L. C.; Prueksaritanont, T.; Shu, C.; Torrent, M.; Heimbrook, D. C.; Kohl, N. E.; Huber, H. E.; Hartman, G. D. *Bioorg. Med. Chem. Lett.* **2006**, *16*, 1775; (c) Garbaccio, R. M.; Fraley, M. E.; Tasber, E. S.; Olson, C. M.; Hoffman, W. F.; Torrent, M.; Buser, C. A.; Walsh, E. S.; Hamilton, K.; Schaber, M. D.; Lobell, R. B.; Tao, W.; South, V. J.; Yan, Y.; Kuo, L. C.; Prueksaritanont, T.; Slaughter, D. E.; Shu, C.; Heimbrook, D. C.; Kohl, N. E.; Huber, H. E.; Hartman, G. D. *Bioorg. Med. Chem. Lett* **2006**, *16*, 1780; (d) Cox, C. D.; Torrent, M.; Breslin, M. J.; Mariano, B. J.; Whitman, D. B.; Coleman, P. J.; Buser, C. A.; Walsh, E. S.; Hamilton, K.; Schaber, M. D.; Lobell, R. B.; Tao, W.; South, V. J.; Kohl, N. E.; Yan, Y.; Kuo, L. C.; Prueksaritanont, T.; Slaughter, D. E.; Li, C.; Mahan, E.; Lu, B.; Hartman, G. D. *Bioorg. Med. Chem. Lett.* **2006**, *16*, 3175; (e) Cox, C. D.; Breslin, M. J.; Whitman, D. B.; Coleman, P. J.; Garbaccio, R. M.; Fraley, M. E.; Buser, C. A.; Walsh, E. S.; Hamilton, K.; Schaber, M. D.; Lobell, R. B.; Tao, W.; Abrams, M. T.; South, V. J.; Davide, J. P.; Kohl, N. E.; Hartman, G. D. *Bioorg. Med. Chem. Lett.* **2007**, *17*, 2697; (f) Coleman, P. J.; Schreier, J. D.; Cox, C. D.; Fraley, M. E.; Garbaccio, R. M.; Buser, C. A.; Walsh, E. S.; Hamilton, K.; Lobell, R. B.; Rickert, K.; Tao, W.; Diehl, R. E.; South, V. J.; Davide, J. P.; Kohl, N. E.; Yan, Y.; Kuo, L.; Salata, J. J.; Hartman, G. D. *Bioorg. Med. Chem. Lett.* **2007**, *previous letter #1*; (g) Garbaccio, R. M.; Tasber, E. S.; Neilson, L.; Coleman, P. J.; Fraley, M. E.; Olson, C.; Bergman, J.; Torrent, M.; Buser, C. A.; Walsh, E. S.; Hamilton, K.; Lobell, R. B.; Tao, W.; South, V. J.; Diehl, R. E.; Davide, J. P.; Yan, Y.; Kuo, L. C.; Li, C.; Prueksaritanont, T.; Slaughter, D. E.; Salata, J. J.; Kohl, N. E.; Huber, H. E.; Hartman, G. D. *Bioorg. Med. Chem. Lett.* **2007**, *previous letter #2*.
2. See also, Coleman, P. J.; Mercer, S. P.; Roecker, A. J. WO 2006 068933 A2.
3. Intermolecular cycloadditions of this type are well precedented in the literature, however, the products either give the undesired regiochemistry for compound **2** or products that are difficult to convert to compounds similar to **2**. See (a) Shimizu, T.; Hayashi, Y.; Nishio, T.; Teramura, K. *Bull. Chem. Soc. Jpn.* **1984**, *57*, 787; (b) Barluenga, J.; Fernandez-Mari, F.; Gonzalez, R.; Aguilar, E.; Revelli, G. A.; Viado, A. L.; Fananas, F. J.; Olano, B. *Eur. J. Org. Chem.* **2000**, *9*, 1773.
4. (a) Lam, P. Y. S.; Clark, C. G.; Saubern, S.; Adams, J.; Winters, M. P.; Chan, D. M. T.; Combs, A. *Tetrahedron Lett.* **1998**, *39*, 2941; (b) Chan, D. M. T.; Monaco, K. L.; Wang, R.-P.; Winters, M. P. *Tetrahedron Lett.* **1998**, *39*, 2933; (c) Evans, D. A.; Katz, J. L.; West, T. R. *Tetrahedron Lett.* **1998**, *39*, 2937.
5. Ritter, T.; Lisbet, K.; Werder, M.; Hauser, H.; Carreira, E. M. *Org. Biomol. Chem.* **2005**, *3*, 3514.
6. Moore, J. A. *J. Org. Chem.* **1955**, *20*, 1607, and references therein.
7. Jacobson, R. M.; Eur. Pat. Appl., **1985**, EP 153127 A2.
8. KSP inhibitory activity was measured using a standard ATPase assay. IC_{50} values are reported as averages of at least two determinations; standard deviations are ±25–50%.
9. Mitotic arrest was measured by assessing the mitosis specific phosphorylation of nucleolin using an antibody-coated, bead-based assay. In this assay, total nucleolin is captured on a streptavidin-coated paramagnetic bead coupled with biotinylated nucleolin monoclonal IgG1 antibody 4E2 (Research Diagnostics, Inc.). Nucleolin phosphorylation is detected by an antibody complex consisting of a phospho-specific nucleolin IgM monoclonal antibody, TG3 (Applied NeuroSolutions, Inc.) and a goat anti-mouse IgM labeled with a ruthenium Tris–bipyridyl complex (BV-TAG Technology, BioVeris Corp.). The complex is quantitated via electrochemiluminescence based on the excitation/emission properties of the Tris–bipyridyl complex using a BioVeris M-series analyzer. EC_{50} for KSP-induced nucleolin phosphorylation was determined after treatment with a compound in a 7-point, half-log dilution series for 16 h. The values of EC_{50} are reported as average of at least two independent determinations; standard deviations are within ±25–50% of EC_{50} values.
10. Separation of **25** was performed on a ChiralPak AD (4.6 mm × 250 mm for analytical; then 250 × 5 cm for preparatory scale, 99:1 hexanes:EtOH, 0.1% diethylamine as a modifier) column to afford analytically pure material (98.5% e.e.). The first isomer to elute was the (−) antipode (R_t = 6.77 min), and it was 'inactive' (KSP IC_{50} = 221 nM). The second isomer to elute was the (+) antipode (R_t = 9.03 min), and it was active (KSP IC_{50} = 0.2 nM). Data for **25**: NMR (500 MHz, $CDCl_3$): δ = 7.39 (dd, J = 8.0, 1.5 Hz, 1H), 7.32–7.28 (m, 4H), 7.24–7.19 (m, 1H), 6.95 (dd, 12.5, 8.5 Hz, 1H), 6.84–6.78 (m, 1H), 4.38 (dd, J = 11.5, 3.5 Hz, 1H), 4.27 (dd, J = 11.5, 3.5 Hz, 1H), 2.47 (s, 3H), 2.46–2.35 (m, 3H), 2.35 (s, 3H), 2.26–2.19 (m, 1H), 2.22 (s, 6H), 1.58–1.49 (m, 1H), 1.34–1.25 (m, 1H) ppm. HRMS (ES) calcd M+H for $C_{23}H_{28}FN_3O$ 382.2294. Found: 382.2289.
11. See Ref. 1a for a discussion of the unique allosteric binding site of KSP. More than 20 structurally related inhibitors have been crystallized in the allosteric binding pocket of KSP and all have had the orientation shown at the relevant stereocenter of **25**. See Ref. 1a for the details of the co-crystallization procedure. The coordinates of the co-crystal structures have been deposited with RCSB Protein Data Bank under the access codes 2Q2Y and 2Q2Z.
12. Relative to the parental KB-3-1 cells, KB-V-1 cells, originally derived by culturing KB-3-1 cells in the presence of the Pgp substrate vinblastine (*J. Biol. Chem.* **1986**, *261*, 7762), express >500-fold higher levels of Pgp mRNA and protein. The compound potency (IC_{50}) for induction of mitotic arrest was determined by evaluating the levels of the mitotic marker phospho-nucleolin after 16 h incubation with the test compound in an 11-point half-log dilution series. The ratio of IC_{50} obtained in KB-V-1 cells vs. that in KB-3-1 cells is defined as the MDR ratio. As a general guideline, we considered compounds with MDR ratios <10 to be of interest for their ability to enter and kill cells that overexpress Pgp. Verapamil, a competitive inhibitor of Pgp, restores the activity of Taxol and our KSP inhibitors in the KB-V-1 cell line to nearly that observed in the parental KB-3-1 line, confirming that Pgp efflux is responsible for the observed resistance to drug-mediated mitotic arrest. All compounds presented in this manuscript have MDR ratios of less than 4.4.

13. The hERG IC_{50} values are reported as averages of at least two independent determinations and were acquired by radioligand binding competition experiments using membrane preparations from human embryonic kidney cells that stably express hERG. For assay details, see: Bilodeau, M. T. et al. *J. Med. Chem.* **2004**, *47*, 6363 and references therein. It should be noted that the ratios of hERG IC_{50}/KSP EC_{50} or hERG IC_{50}/KSP EC_{99} could also be used to determine off-target window. Compound **1** has approximately a twofold better ratio than compound **25** via this analysis.
14. Athymic nude mice (nu/nu) were xenografted subcutaneously with the human ovarian carcinoma cell line A2780 and the resulting tumors were allowed to reach 200–300 mm^3 before mice were surgically implanted with Alzet minipumps (Durect Corporation) filled with the appropriate KSP inhibitors according to manufacturer's recommendations. Prior to the implant, pumps containing KSP inhibitors were primed by incubation in 37 °C water bath for 3 h, so that the pumps would discharge KSP inhibitors at a constant rate of 8 μL/h after subcutaneous implantation. Mice were euthanized 22 h post pump implant and blood and tumors were harvested. Blood was collected in EDTA Vacutainers and processed for plasma to determine pharmacokinetics. Tumors were fixed in 10% neutral buffered formalin and then processed and embedded in paraffin. Paraffin embedded tumors were sectioned 5 μm thick and used in a phospho-histone H3 immunohistochemistry assay designed to determine the percentage of cells blocked in mitosis compared to control treated tumors. After paraffin removal, re-hydration, and antigen retrieval, sections were incubated with anti-phospho-histone H3 (ser10; Upstate). Following incubation with a biotinylated secondary antibody, staining of antigen positive nuclei was accomplished using avidin:biotin complexed horseradish peroxidase and diaminobenzidine reagent. Sections were imaged using an Olympus BX51 microscope with a motorized stage and Image-Pro Analysis software. Quantization of the sections was accomplished by measuring the percentage of positively stained nuclei (black) per unit area.